A FINITE LINE CRACK IN A PRESSURIZED SPHERICAL SHELL

Efthymios S. Folias*

ABSTRACT

The deformation of a thin sheet having initial spherical curvature is shown to be associated with that of an initially flat plate resting upon an elastic foundation. Using an integral formulation the coupled Reissner equations for a shell with a crack of length 2c are solved for the in-plane and Kirchhoff bending stresses, and, among other things, it is found that the explicit nature of the stresses near the crack point depends upon the inverse half power of the non-dimensional distance from the point ε. The character of the combined extension-bending stress field near the crack tip is investigated in detail for the special case of a radial crack in a spherical cap which is subjected to a uniform internal pressure q_o and is clamped at the boundary $\bar{R} = \bar{R}_o$. Pending a complete study of the solution, approximate results for the combined surface stresses near the crack tip normal and along the line of crack prolongation are respectively of the form

$$\sigma_y(\varepsilon,0)\Big|_{\substack{\nu=1/3\\ \lambda=0.98\\ c=0.23\text{ in}\\ \bar{R}_o=4.25\text{ in}}} \approx 0.45\sqrt{1/\varepsilon}\,\frac{q_oR}{h} + \ldots$$

and similarly

$$\sigma_x(\varepsilon,0)\Big|_{\substack{\nu=1/3\\ \lambda=0.98\\ c=0.23\text{ in}\\ \bar{R}_o=4.25\text{ in}}} \approx 0.45\sqrt{1/\varepsilon}\,\frac{q_oR}{h} + \ldots$$

It is interesting to note that the stress σ_x and σ_y, along the line of crack prolongation, for this geometry are equal. In general, they will be of the same sign and will differ only slightly in magnitude due to the bending component. Finally, the experimental and theoretical results for ε_y, along the line of crack prolongation, compare very well.

INTRODUCTION

In the field of fracture mechanics, considerable work has been carried out on initially flat sheets subjected to either extensional or bending stresses, and for small deformations the superposition of these separate effects [1] is permissible. On the other hand, if a thin sheet possesses initial curvature, a bending load will generally produce both bending and extensional stresses, and vice versa. The subject of eventual concern therefore is that of the simultaneous stress fields produced in an initially curved sheet containing a crack.

It is of some practical value to be able to correlate flat sheet behavior with that of initially curved specimens. In experimental work, for example, considerable time could be saved if a reliable prediction of curved sheet response behavior could be made from flat sheet tests. For this reason an exploratory study was undertaken to assess analytically the manner in which the two problems might be related. Although it is recognized that elastic analysis is not completely satisfactory due to plastic flow near the crack tip, considerable information can be obtained.

Two initially curved geometries immediately come to mind: a spherical shell and a cylindrical shell. In the latter case one

* Formerly Research Fellow, California Institute of Technology, Dr. Folias is currently in Thessaloniki, Greece. Mailing address c/o the editorial office, Pasadena, California.

of the principal radii of curvature is infinite and the other constant. It might appear therefore that this geometric simplicity leads to a rather straightforward analytical solution. However, the fact that the curvature varies between zero and a constant as one considers different angular positions -- say around the point of a crack which is aligned parallel to the cylinder axis -- more than obviates the initial geometric simplification and therefore increases the mathematical complexities considerably. For this reason, Sechler and Williams [2] suggested an approximate equation, based upon the behavior of a beam on an elastic foundation, and were able to obtain a reasonable agreement with the experimental results. Since then, the present author has investigated this problem in a more sophisticated manner and has obtained a solution which will be reported separately. In this paper, a spherical section of a large radius of curvature constant in all directions is chosen for consideration.

CRACKED SPHERICAL SHELL

Formulation of the Problem

Consider a segment of a thin, shallow* spherical shell of constant thickness h and subjected to an internal pressure q(X, Y). The material of the shell is assumed to be homogeneous and isotropic and at the apex there exists a radial cut of length 2c oriented symmetrically with respect to the apex. Following Reissner [3], the coupled differential equations governing the bending deflection W(X, Y) and the membrane stress function F(X, Y), with X, Y as rectangular coordinates of the base plane (see Fig. 1), are given by:

$$-\frac{Eh}{R}\nabla^2 W(X,Y) + \nabla^4 F(X,Y) = 0 \tag{1}$$

$$\nabla^4 W(X,Y) + \frac{1}{RD}\nabla^2 F(X,Y) = \frac{q(X,Y)}{D} \tag{2}$$

It is convenient at this point to introduce dimensionless coordinates, namely

$$x \equiv \frac{X}{c}, \qquad y \equiv \frac{Y}{c} \tag{3}$$

which change the homogeneous parts of (1) and (2) to:

$$-\frac{Ehc^2}{R}\nabla^2 W + \nabla^4 F = 0 \tag{4}$$

$$\nabla^4 W + \frac{c^2}{RD}\nabla^2 F = 0 \tag{5}$$

As to boundary conditions, one must now require that the normal moment, equivalent vertical shear, and normal and tangential inplane stresses vanish along the crack. However, suppose that

* A segment will be called shallow if the ratio of height to base diameter is less than, say, 1/8.

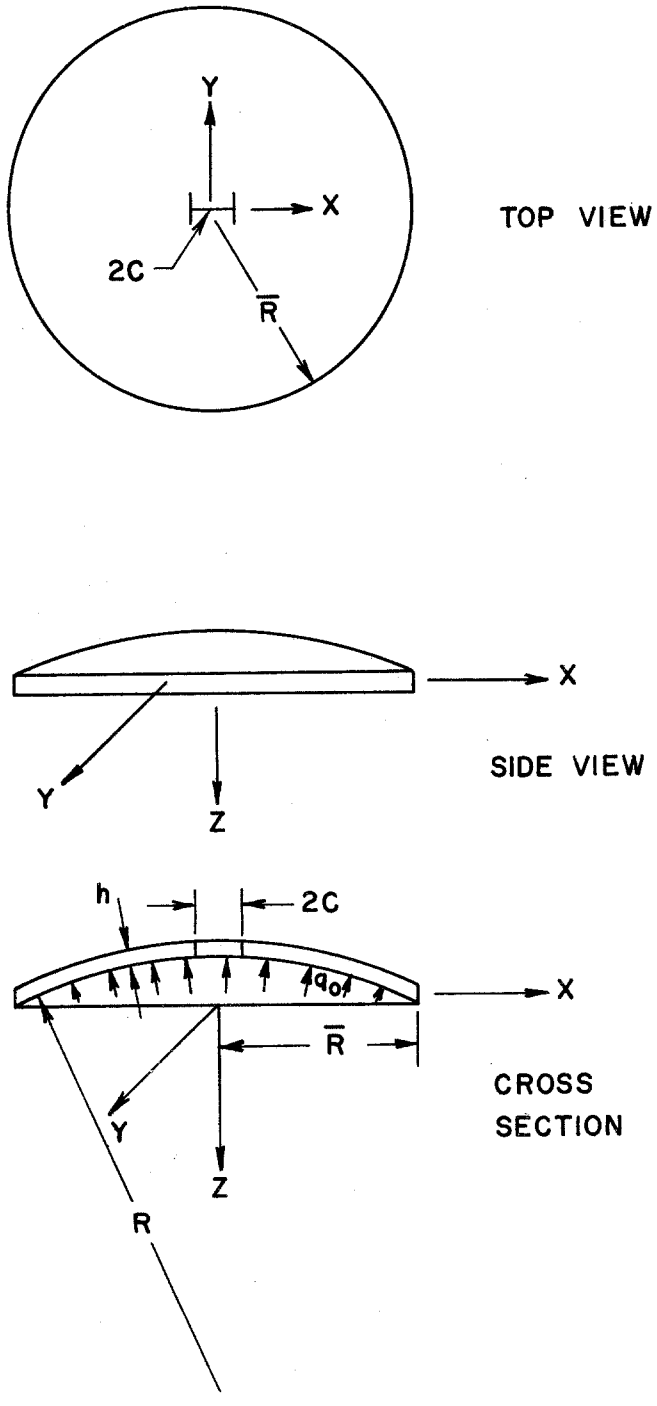

Fig. 1. Geometry and Coordinates.

one has already found* a particular solution satisfying 4 and 5, but producing a residual normal moment M_y, equivalent vertical shear V_y, normal in-plane stress N_y, and an in-plane

* See the next section for an example.

tangential stress N_{xy}, along the real axis $|x| < 1$, of the form:

$$M_y^{(P)} = -\frac{D}{c^2} m(x) \tag{6}$$

$$V_y^{(P)} = -\frac{D}{c^2} v(x) \tag{7}$$

$$N_y^{(P)} = -\frac{n(x)}{c^2} \tag{8}$$

$$N_{xy}^{(P)} = -\frac{t(x)}{c^2} \tag{9}$$

Thus we need to find two functions of the dimensionless coordinates (x, y), $W(x, y)$ and $F(x, y)$, such that they satisfy the partial differential equations 4 and 5 and the following boundary conditions. At $y = 0$ and $|x| < 1$

$$M_y(x, 0) = -\frac{D}{c^2}\left[\frac{\partial^2 W}{\partial y^2} + \nu \frac{\partial^2 W}{\partial x^2}\right] = \frac{D}{c^2} m(x) \tag{10}$$

$$V_y(x, 0) = -\frac{D}{c^3}\left[\frac{\partial^3 W}{\partial y^3} + (2 - \nu) \frac{\partial^3 W}{\partial x^2 dy}\right] = \frac{Dv(x)}{c^3} \tag{11}$$

$$N_y(x, 0) = \frac{1}{c^2} \frac{\partial^2 F}{\partial x^2} = \frac{n(x)}{c^2} \tag{12}$$

$$N_{xy}(x, 0) = -\frac{1}{c^2} \frac{\partial^2 F}{\partial x \partial y} = \frac{t(x)}{c^2} \tag{13}$$

At $y = 0$ and $|x| > 1$, we must satisfy the continuity requirements, namely:

$$\lim_{|y| \to 0} \left[\frac{\partial^n}{\partial y^n}(W^+) - \frac{\partial^n}{\partial y^n}(W^-)\right] = 0 \tag{14}$$

$$\lim_{|y| \to 0} \left[\frac{\partial^n}{\partial y^n}(F^+) - \frac{\partial^n}{\partial y^n}(F^-)\right] = 0 \tag{15}$$

$$(n = 0, 1, 2, 3).$$

Furthermore, because we are limiting our selves to a large radius of curvature for this shallow shell, i.e., small deviations from a flat sheet, we can apply certain boundary conditions at infinity even though we know physically that the stresses and displacements far away from the crack are finite. Therefore, to avoid infinite stresses and infinite displacements we must require that the displacement function W and the stress function F with their first derivatives to be finite far away from the

crack. These restrictions simplify the mathematical complexities of the problem considerably, and correspond to the usual expectations of the St. Venant Principle. It should be pointed out that the boundary conditions at infinity are not geometrically feasible. However if the crack is small compared to the dimensions of the shell, the approximation is good.

Method of Solution

Reissner [4] has shown that the solution of the system 4, 5 can be written in the form

$$W = \chi + \Phi \tag{16}$$

$$F = -\frac{RD}{c^2}\nabla^2\chi + \psi \tag{17}$$

where Φ and ψ are harmonic functions and χ satisfies the same differential equation as the deflection of a plate on an elastic foundation, i.e.

$$(\nabla^4 + \lambda^4)\,\chi = 0 \tag{18}$$

where

$$\lambda^4 \equiv \frac{Ehc^4}{R^2D} \equiv \frac{12(1-\nu^2)}{(\frac{R}{h})^2}\,(\frac{c}{h})^4 \tag{19}$$

The function ψ represents the inextensional bending part of the solution, and Φ represents the membrane part of the solution. We next construct the integral representations

$$W(x, y^{\pm}) = \int_0^{\infty}\{P_1 e^{-\sqrt{s^2-i\lambda^2}|y|} + P_2 e^{-\sqrt{s^2+i\lambda^2}|y|} + P_3 e^{-s|y|}\}\cos xs\,ds \tag{20}$$

$$F(x, y^{\pm}) = \frac{i\lambda^2 RD}{c^2}\int_0^{\infty}\{P_1 e^{-\sqrt{s^2-i\lambda^2}|y|} - P_2 e^{-\sqrt{s^2+i\lambda^2}|y|} + P_4 e^{-s|y|}\}\cos xs\,ds \tag{21}$$

where the P_i $(i = 1, 2, 3, 4)$ are arbitrary functions of s to be determined from the boundary conditions, and the $\pm$ signs refer to $y > 0$ and $y < 0$ respectively. In reference [5], it is shown that the problem is reduced to the solution of two coupled singular integral equations which, because of the complicated nature of the kernels, are solved for small values of the parameter λ. This is certainly permissible since for most practical applications the parameter λ attains small values as follows from the definition of λ, namely

$$\lambda \equiv \sqrt[4]{12(1-\nu^2)}\,(\frac{c}{R})\cdot(\frac{R}{h})^{\frac{1}{2}} \tag{22}$$

It is clear that λ is small for large ratios of R/h and small crack lengths. As a practical matter, if we consider crack

lengths less than one tenth of the periphery, i.e. $2c < \frac{2\pi R}{10}$, and for $R/h < 10^3$ a corresponding upper bound for λ can be obtained, namely $\lambda < 20$. Thus the range of λ becomes $0 < \lambda < 20$ and for most practical cases is between 0 and 2.

Finally, without going into the details we obtain the displacement function W and the stress function F (see appendix) for $m = m_o$, $v = 0$, $n = n_o$ and $t = 0$.* Thus the stresses are found to be:

*Bending stresses:*** On the surface $Z = + \frac{h}{2}$

$$\sigma_{x_b} = - \frac{Eh}{2(1+\nu)c^2} \frac{\tilde{P}_{10}}{\sqrt{\epsilon}} \left(\frac{3}{4} \cos \frac{\theta}{2} + \frac{1}{4} \cos \frac{5\theta}{2}\right) + O(\epsilon^0) \tag{23}$$

$$\sigma_{y_b} = \frac{Eh}{2(1-\nu^2)c^2} \frac{\tilde{P}_{10}}{\sqrt{\epsilon}} \left(\frac{11+5\nu}{4} \cos \frac{\theta}{2} + \frac{1-\nu}{4} \cos \frac{5\theta}{2}\right) + O(\epsilon^0) \tag{24}$$

$$\tau_{xy_b} = - \frac{Gh}{(1-\nu)c^2} \frac{\tilde{P}_{10}}{\sqrt{\epsilon}} \left(\frac{7+\nu}{4} \sin \frac{\theta}{2} + \frac{1-\nu}{4} \sin \frac{5\theta}{2}\right) + O(\epsilon^0) \tag{25}$$

where

$$\tilde{P}_{10} \equiv \alpha^2 \lambda^2 \frac{A_1 - B_1}{2\sqrt{2}} = - \frac{n_o \lambda^2}{\sqrt{2EhD}(4-\nu_o)} \left\{\frac{8-7\nu_o}{32} + \frac{4-3\nu_o}{8} \gamma + \right.$$

$$\left. \frac{4-3\nu_o}{16} \left(1 + \ell n \frac{\lambda^2}{16}\right)\right\} + \frac{m_o}{\sqrt{2}(4-\nu_o)} \left\{1 + \frac{\pi\lambda}{32} \frac{4-3\nu_o}{4-\nu_o}\right\} + O(\lambda^4 \ell n \lambda) \tag{26}$$

Similarly

Extensional stresses:

$$\sigma_{x_e} = \frac{\tilde{P}_{20}}{hc^4 \sqrt{\epsilon}} \left(\frac{3}{4} \cos \frac{\theta}{2} + \frac{1}{4} \cos \frac{5\theta}{2}\right) + O(\epsilon^0) \tag{27}$$

$$\sigma_{y_e} = \frac{\tilde{P}_{20}}{hc^4 \sqrt{\epsilon}} \left(\frac{5}{4} \cos \frac{\theta}{2} - \frac{1}{4} \cos \frac{5\theta}{2}\right) + O(\epsilon^0) \tag{28}$$

$$\tau_{xy_e} = - \frac{\tilde{P}_{20}}{hc^4 \sqrt{\epsilon}} \left(\frac{1}{4} \sin \frac{\theta}{2} - \frac{1}{4} \sin \frac{5\theta}{2}\right) + O(\epsilon^0) \tag{29}$$

* Reference [5] also discusses the method of solution for the case that m and n are functions of x. The case of $v \neq 0$ and $t \neq 0$ is discussed in reference [6].

** Note because of the Kirchhoff boundary conditions, the bending shear stress does not vanish in the free edge. For the flat sheet this problem was discussed by Knowles and Wang [7].

where

$$\tilde{P}_{20} \equiv \frac{\lambda^4 RD}{2\sqrt{2}} (A_1 + B_1)$$

$$= \frac{n_o c^2}{\sqrt{2}}\{1 + \frac{3\pi}{32}\lambda^2\} + \frac{m_o \lambda^2 \sqrt{EhD}\, c^2}{\sqrt{2}\,(4-\nu_o)}\{\frac{13}{32} + \frac{3\gamma}{8} + \frac{3}{16}\ell n \frac{\lambda^2}{16}\} \quad (30)$$

$$+ O(\lambda^4 \ell n\lambda).$$

It is apparent from the above expressions that there exists an interaction between bending and stretching, except that in the limit as $\lambda \to 0$ the stresses of a flat sheet are recovered and coincide with those obtained previously for bending [8] and extension [9]. Thus the local stresses in a shell are expressed in terms of the local stresses in a flat sheet.

Combined stresses:

In general, the combined stresses will depend upon the contributions of the particular solutions reflecting the magnitude and distribution of the applied normal pressure. On the other hand, the singular part of the solution, that is the terms producing (mathematically) infinite elastic stresses at the crack tip, will depend only upon the local stresses existing along the locus of the crack before it is cut, which of course are precisely the stresses which must be removed or cancelled by the particular solutions described above in order to obtain the stress free edges as required physically. Hence the distribution q(x, y) does not -- to the first order -- affect the local character of the stresses at the crack point.

A PARTICULAR SOLUTION

As an illustration of how the local solution may be combined in a particular case, consider a clamped segment of a shallow spherical shell of base radius $\bar{R}_o$ and containing at the apex a finite radial crack of length 2c in the direction of the X-axis (see fig. 2). The shell is subjected to uniform internal pressure

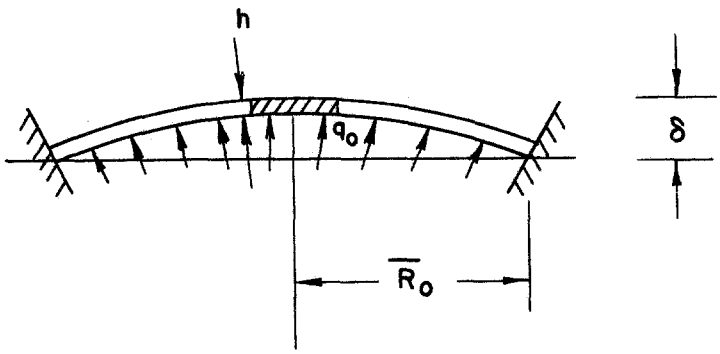

Fig. 2. Clamped spherical cap: A particular case.

q_o with radial extensional stress $N_r = \frac{1}{2} q_o R$, and because it is clamped we require that the displacement and slope vanish at $\bar{R} = \bar{R}_o$. For this problem, Reissner [10] gives the solution of the coupled-extention-bending equations for the uncracked shell as:

$$W_p(r) = C_1 \text{ ber}(\lambda r) + C_2 \text{ bei}(\lambda r) + C_3 \tag{31}$$

$$F_p(r) = \frac{Eh^2}{\sqrt{12(1-\nu^2)}}\{C_1 \text{ bei}(\lambda r) - C_2 \text{ ber}(\lambda r)\} - \frac{1}{4} q_o R r^2 \tag{32}$$

where

$$C_1 = \frac{C^2 q_o R \sqrt{12(1-\nu^2)}\, r_o}{Eh^2 \lambda} \frac{\text{bei}'(\lambda r_o)}{[\text{bei}'(\lambda r_o)]^2 + [\text{ber}'(\lambda r_o)]^2}$$

$$C_2 = -C_1 \left\{\frac{\text{ber}'(\lambda r_o)}{\text{bei}'(\lambda r_o)}\right\}$$

$$C_3 = -C_1 \left\{\frac{\text{ber}(\lambda r_o)\text{bei}'(\lambda r_o) - \text{bei}(\lambda r_o)\text{ber}'(\lambda r_o)}{\text{bei}'(\lambda r_o)}\right\}$$

Along any radial ray, and in particular along $\theta = 0, \pi$, the bending and extensional shear vanish by symmetry, and the circumferential bending and stretching stresses are

$$M_{\theta\theta}^{(P)}(r) = \frac{D\lambda^2}{c^2}\{C_1[\nu \text{bei}(\lambda r) - (1-\nu)\frac{\text{ber}'(\lambda r)}{r}]$$

$$-C_2[\nu \text{ber}(\lambda r) + (1-\nu)\frac{\text{bei}'(\lambda r)}{\lambda r}]\} \tag{33}$$

$$N_{\theta\theta}^{(P)}(r) = \frac{Eh^2(\lambda^2/c^2)}{\sqrt{12(1-\nu^2)}}\{C_1 \text{ bei}''(\lambda r) - C_2 \text{ ber}''(\lambda r)\} - \tfrac{1}{2} q_o R \tag{34}$$

$$N_{r\theta}(r) = 0 \tag{35}$$

$$V_{r\theta}(r) = 0 \tag{36}$$

Therefore, the homogeneous solution must negate these values from the particular solution. But since we already have obtained a solution for uniform loading along the crack, namely m_o and n_o, therefore we will make use of these results in order to obtain an estimate of the stresses in the vicinity of the crack. As an engineering approximation, by considering an upper and lower bound on m_o and n_o, we may estimate an upper and lower bound for the stresses in the neighborhood of the crack point. On the other hand, if we are interested in the stresses away from the crack, say three times the crack length, then by Saint Venant's principle we need to take only the average values. Thus we define

$$\frac{Dm_o^{(\ell)}}{c^2} = \min_{|x|<1,\theta=0} M_{\theta\theta}^{(P)} \leqslant \frac{Dm_{true}}{c^2} \leqslant \max_{|x|<1,\theta=0} M_{\theta\theta}^{(P)} = D\frac{m_o^{(u)}}{c^2}$$

and similarly

$$\frac{n_o^{(\ell)}}{c^2} = \min_{|x|<1,\theta=0} N_{\theta\theta}^{(P)} \leqslant \frac{n_{true}}{c^2} \leqslant \max_{|x|<1,\theta=0} N_{\theta\theta}^{(P)} = \frac{n_o^{(u)}}{c^2}$$

Next, let us consider a spherical shell with the following geometrical dimensions:

$$\begin{aligned} \bar{R}_o &= 4.25 \\ R &= 20 \text{ in.} \\ h &= 0.009 \text{ in.} \\ \nu &= 1/3 \\ 2c &= 0.46 \text{ in.} \\ E &= 16 \times 10^6 \text{ psi} \end{aligned}$$

from which we can calculate the parameters

$$\begin{aligned} \lambda &= 0.98 \\ r_o &= 18.50 \end{aligned}$$

The following table shows the variation of the residual moment $M_{\theta\theta}^{(P)}$ and membrane force $N_{\theta\theta}^{(P)}$ along the crack.

X	$\lambda x = \lambda\frac{X}{c}$	$N_{\theta\theta}^{(P)}$	$M_{\theta\theta}^{(P)}$
0	0	$-0.50\ q_oR$	$0.89 \times 10^{-4}\ q_oRh$
0.074	0.30	$-0.50\ q_oR$	$0.87 \times 10^{-4}\ q_oRh$
0.117	0.50	$-0.50\ q_oR$	$0.92 \times 10^{-4}\ q_oRh$
0.164	0.70	$-0.50\ q_oR$	$0.94 \times 10^{-4}\ q_oRh$
0.235	1.00	$-0.50\ q_oR$	$0.97 \times 10^{-4}\ q_oRh$
		diff. 0%	diff. 9%

It is clear from the table above that $M_{\theta\theta}^{(P)}$ and $N_{\theta\theta}^{(P)}$ are almost uniform along the crack. Therefore we may choose

$$\frac{n_o^{(u)}}{c^2} = 0.50\ q_o\ R$$

$$\frac{Dm_o^{(u)}}{c^2} = -0.97 \times 10^{-4}\ q_o\ Rh$$

Returning now to the stresses along the line of crack prolongation, for example the normal stress $\sigma_{y_{total}}(X, 0)$, one finds using 24 and 28 that:

$$\sigma_{y_{total}}(X,0)\Big|_{\nu=1/3} \approx \frac{\overline{\sigma}_b}{\sqrt{2(X-1)/c}}\{1+(0.16+0.03\ \ell n\frac{\lambda^2}{16})\lambda^2\} \tag{37}$$

$$+\frac{\overline{\sigma}_e}{\sqrt{2(X-1)/c}}\{1-(0.38+0.23\ \ell n\frac{\lambda^2}{16})\lambda^2\}$$

which for $\lambda = 0.98$ reduces to:

$$\sigma_{y_{total}}(X,0) \approx \frac{\overline{\sigma}_b}{\sqrt{2(X-1)/c}}\{1.07\}+\frac{\overline{\sigma}_e}{\sqrt{2(X-1)/c}}\{1.27\} \tag{38}$$

where

$$\overline{\sigma}_b = \frac{6D}{h^2}\frac{m_o}{c^2} = \text{"applied bending"}$$

$$\overline{\sigma}_e = \frac{n_o}{c^2 h} = \text{"applied stretching"}$$

And for our particular example, we can associate

$$\overline{\sigma}_b^{(u)} \approx -0.58\times 10^{-3}\frac{q_o R}{h} = -0.001\frac{q_o R}{h} \tag{39}$$

$$\overline{\sigma}_e^{(u)} \approx 0.50\frac{q_o R}{h} \tag{40}$$

From equation 38 we see that the initial curvature will increase the applied bending stress in this case by approximately 7% and the applied stretching stress by 27%. One deduces therefore that the critical crack length of a shell decreases with an increase of λ or a decrease of radius of curvature. In this particular case it is found that the direct bending stresses are negligible compared to the extensional ones and the combined stress is

$$\sigma_{y_{total}}(X,0)\Big|_{\nu=1/3} \approx \frac{0.64}{\sqrt{\frac{2(X-1)}{c}}}\frac{q_o R}{h} = \frac{0.64\sqrt{c}}{\sqrt{2(X-1)}}\frac{q_o R}{h} \tag{41}$$

$$\sigma_{x_{total}}(X,0)\Big|_{\nu=1/3} \approx \frac{0.64\sqrt{c}}{\sqrt{2(X-1)}}\frac{q_o R}{h} \tag{42}$$

where, based on the Kirchhoff theory, the two-dimensional "hydrostatic tension" nature of the σ_x and σ_y stresses predicted for flat plates is preserved. Finally, the corresponding strains are

$$\epsilon_y(X,0) \approx 0.30\sqrt{\frac{c}{X-1}}\ \frac{q_o R}{Eh} \tag{43}$$

$$\epsilon_x(X,0) \approx 0.30\sqrt{\frac{c}{X-1}}\ \frac{q_o R}{Eh} \tag{44}$$

GRIFFITH'S THEORY OF FRACTURE FOR CURVED SHEETS

As is well known in fracture mechanics, the prediction of failure in the presence of sharp discontinuities is a very complicated problem. Some work has been done on flat sheets, based on the brittle fracture theory of A. A. Griffith [11]. His hypothesis is that the total energy of a cracked system subjected to loading remains constant as the crack extends an infinitesimal distance. It should of course be recognized that this is a necessary condition for failure but not sufficient.

Griffith applied his criterion to an infinite, isotropic plate containing a flat, sharp-ended crack of length 2c. We shall now proceed to obtain a similar, but approximate, criterion for initially curved sheets based upon only the singular terms of the stresses.

The basic concept for crack instability is

$$\frac{\partial U_{system}}{\partial c} = 0 \tag{45}$$

where the system energy is defined by

$$U_{system} = U_{loading} + U_{strain} + U_{surface} \tag{46}$$

The applied stresses are held constant so that

$$U_{loading} = U_o - h\int_P (\sigma_\xi u_\eta + \tau_{\xi\eta} u_\eta)\ dP \tag{47}$$

where U_o is a reference constant energy, and the integration is over that portion of the outer perimeter where forces act to cause displacements. The strain energy is

$$U_{strain} = \tfrac{1}{2}\int_{vol} (\sigma_\xi \epsilon_\xi + \tau_{\xi\eta}\gamma_{\xi\eta} + \sigma_\eta \epsilon_\eta)\ d\ vol. \tag{48}$$

$$U_{surface} = \gamma(2S + Ph + 4ch) \tag{49}$$

It may be shown that the surface area S of the shell faces and the outer perimeter P of the shell are independent of the crack length.

Therefore 46 may be written as

$$\begin{aligned} U_{system} = {} & U_o' + 4\gamma^* hc - h\int_P (\sigma_\xi u_\xi + u_\eta \tau_{\xi\eta})dP \\ & + \tfrac{1}{2}\int_{vol} (\sigma_\xi \epsilon_\xi + \tau_{\xi\eta}\gamma_{\xi\eta} + \sigma_\eta \epsilon_\eta)\ d\ vol. \end{aligned} \tag{50}$$

or

$$U_{system} = U_o' + 4\gamma^* c -$$

$$-\lim_{\varepsilon \to 0} \frac{c}{8G} \int_{Z_1}^{Z_2} \int_{\varepsilon}^{A^*} \int_{-\pi}^{\pi} \{\frac{1-\nu}{1+\nu}(\sigma_r+\sigma_\theta)^2+(\sigma_r-\sigma_\theta)^2+(2\tau_{r\theta})^2\}R^* dR^* d\theta dZ$$

where $U_o' = U_o + \gamma^* (2A + Ph)$, $Z_1 = Z_o - \frac{h^*}{2}$, $Z_2 = Z_o + \frac{h^*}{2}$ and A^* a radius to be determined (see fig. 3). In the above we have defined

$$\frac{h^*}{2} = R\left[\sqrt{1-\left(\frac{R-h/2}{R}\right)^2 \frac{\bar{R}^2}{R^2}} - \frac{R-h/2}{R}\sqrt{1-\frac{\bar{R}^2}{R^2}}\right]$$

$$Z_o = \sqrt{R^2 - \bar{R}^2} - (R-\delta)$$

with δ the height of the shell segment.

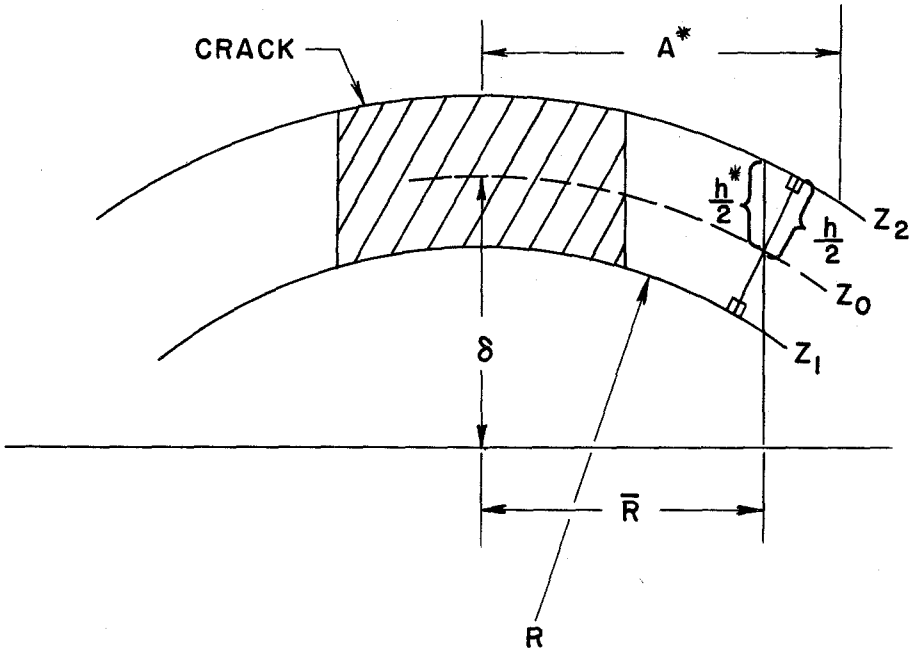

Fig. 3. Geometric details for fracture criterion.

Integration of 50 with respect to θ gives:

$$U_{system} = U_o' + 4\gamma^* ch - \lim_{\varepsilon \to 0} \frac{c}{8G} \int_{Z_1}^{Z_2} \int_{\varepsilon}^{A^*} I_1 dR^* dZ \qquad (51)$$

where

$$I_1 = \frac{1-\nu}{1+\nu}[(K_0+K_2)^2+(K_1+K_3)^2]+[(K_0-K_2)^2+(K_1-K_3)^2] \tag{52}$$

with

$$K_0-K_2 = \frac{EZ}{2c^2}\frac{7+\nu}{1-\nu^2}\tilde{P}_{10} - \frac{1}{2h}\frac{\tilde{P}_{20}}{c^4} \tag{53}$$

$$K_0+K_2 = \frac{EZ}{c^2}\frac{2\tilde{P}_{10}}{(1-\nu)} + \frac{2}{h}\frac{\tilde{P}_{20}}{c^4} \tag{54}$$

$$K_1+K_3 = 0 \tag{55}$$

$$K_1-K_3 = -\frac{EZ}{(1+\nu)}\frac{\tilde{P}_{10}}{2c^2} + \frac{1}{2h}\frac{\tilde{P}_{20}}{c^4} \tag{56}$$

And since we are restricting ourselves to the singular stresses, it is only fair to derive a Griffith criterion applicable in the immediate neighborhood of the crack tip, where because locally the shell is almost flat, we can replace without much error the limits of integration Z_1 and Z_2 by $-\frac{h}{2}$ and $\frac{h}{2}$. Thus 51 may be approximated by

$$U_{system} = U_o' + 4\gamma^* ch - \lim_{\varepsilon\to 0}\frac{c\pi}{8G}\int_{-h/2}^{h/2}\int_{\varepsilon}^{A^*} I_1 dR^* dZ \tag{57}$$

and after integration

$$\begin{aligned} U_{system} &= U_o' + 4\gamma^* ch \\ &- \frac{c\pi}{8G}\{\frac{1-\nu}{1+\nu}(\frac{2E\tilde{P}_{10}}{c^2(1-\nu)})^2\frac{2}{3}(\frac{h}{2})^3 + \frac{1-\nu}{1+\nu}(\frac{2}{h}\frac{\tilde{P}_{20}}{c^4})^2 h \\ &+ \frac{\nu^2+6\nu+25}{3(1-\nu^2)^2}\frac{E^2\tilde{P}_{10}^{\,2}}{c^4}(\frac{h}{2})^3 + \frac{1}{2}\frac{\tilde{P}_{20}^{\,2}}{h^2c^8}h\} A^* \end{aligned} \tag{58}$$

which in the limit, as $R\to\infty$ and $\bar{\sigma}_b\to 0$, in equal biaxial tension $\bar{\sigma}_e$ along the periphery of a flat sheet, must be equal to (see ref. [12])

$$U_{system} = U_o' + 4\gamma^* ch - \frac{Sh}{4G}(k-1)\bar{\sigma}_e^{\,2} - \frac{\pi c^2 h}{8G}(3-k)\bar{\sigma}_e^{\,2} \tag{59}$$

Thus we have determined the value for A^*, namely

$$A^* = \frac{16\nu c}{9-7\nu} + \frac{16(1-\nu)}{9-7\nu}\frac{S}{\pi c} \tag{60}$$

Substituting in 58 for A^* and applying the basic condition 45, the fracture criterion is seen to be:

$$4\gamma^* h - \frac{\pi c}{4G}\left\{\frac{33+6\nu-7\nu^2}{(1-\nu^2)^2}\,\frac{24}{}\,\frac{E^2\tilde{P}_{10}^{\,2}h^3}{c^4} + \right.$$

$$\left. + \frac{9-7\nu}{2(1+\nu)}\,\frac{\tilde{P}_{20}^{\,2}}{hc^8}\right\}\frac{16\nu}{9-7\nu} = 0 \qquad (61)$$

where

$$\tilde{P}_{10} = -\frac{c^4 h\,\bar{\sigma}_e}{\sqrt{2}\,RD(4-\nu_o)}\left\{\frac{16-13\nu_o}{32} + \frac{4-3\nu_o}{8}\left(\gamma + \ell n\frac{\lambda}{4}\right)\right\}$$

$$+ \frac{h^2c^2\bar{\sigma}_b}{6\sqrt{2}\,(4-\nu_o)D}\left\{1 + \frac{\pi}{32}\,\frac{4-3\nu_o}{4-\nu_o}\,\lambda^2\right\} + 0\,(\lambda^4 \ell\, n\lambda) \qquad (62)$$

and

$$\tilde{P}_{20} = \frac{c^4 h\,\bar{\sigma}_e}{\sqrt{2}}\left\{1 + \frac{3\pi}{32}\lambda^2\right\} + \frac{h^2c^2\lambda^4 R\,\bar{\sigma}_b}{6\sqrt{2}\,(4-\nu_o)}\left\{\frac{13}{32} + \frac{3}{8}\left(\gamma + \ell n\frac{\lambda}{4}\right)\right\} + O(\lambda^4 \ell n\lambda) \qquad (63)$$

Finally introducing 62 and 63 into 62 we arrive after some rearrangement at:

$$\frac{(33+6\nu-7\nu^2)4\nu}{3(9-7\nu)(4-\nu_o)^2}\left(1 + \frac{\pi}{16}\,\frac{4-3\nu_o}{4-\nu_o}\,\lambda^2\right)\bar{\sigma}_b^{\,2} + \frac{4\nu}{1+\nu}\left(1 + \frac{3\pi}{16}\lambda^2\right)\bar{\sigma}_e^2$$

$$+ \left[-\frac{8}{3}\,\frac{(33+6\nu-7\nu^2)\nu}{\sqrt{1-\nu^2}\,(9-7\nu)(4-\nu_o)^2}\left(\frac{16-3\nu_o}{32} + \frac{4-3\nu_o}{8}\,\gamma + \frac{4-3\nu_o}{8}\,\ell n\frac{\lambda}{4}\right) + \right.$$

$$\left. + \frac{8\nu}{\sqrt{3}}\sqrt{\frac{1-\nu}{1+\nu}}\,\frac{1}{(4-\nu_o)}\left(\frac{13}{32} + \frac{3}{8}\,\gamma + \frac{3}{8}\,\ell n\frac{\lambda}{4}\right)\right]\lambda^2\bar{\sigma}_e\,\bar{\sigma}_b = \frac{16G\gamma^*}{\pi c} \qquad (64)$$

which, for the case of a flat sheet, i.e. $\lambda = 0$, reduces to the following simple form:

$$\frac{(33+6\nu-7\nu^2)4\nu}{3(4-\nu_o)^2(9-7\nu)}\,\bar{\sigma}_b^{\,2} + \frac{4\nu}{1+\nu}\,\bar{\sigma}_e^{\,2} = \frac{16G\gamma^*}{\pi c_p} \equiv (\sigma_p^*)^2 \qquad (65)$$

For $\nu = \frac{1}{3}$ equation 64 becomes

$$0.21\,(1 + 0.12\lambda^2)\,\bar{\sigma}_b^2 + (1 + 0.59\,\lambda^2)\,\bar{\sigma}_e^2$$

$$- (0.24 + 0.07\,\ell n\frac{\lambda}{4})\,\lambda^2\,\bar{\sigma}_e\,\bar{\sigma}_b = \frac{16G\gamma^*}{\pi c} \equiv (\sigma_s^*)^2 \qquad (66)$$

which clearly represents a family of ellipses. In view of 66 we can obtain a relation between the critical crack length in a shell and the critical crack length in a plate, i.e. for $\nu = \frac{1}{3}$

$$(\ell_{cr})_{Shell} = \frac{[0.21\ \bar{\sigma}_b^2 + \bar{\sigma}_e^2]_{Plate}\ (\ell_{cr})_{Plate}}{[0.21(1+0.12\lambda^2)\bar{\sigma}_b^2+(1+0.59\lambda^2)\bar{\sigma}_e^2-(0.24+0.07\ell n\frac{\lambda}{4})\lambda^2\bar{\sigma}_e\bar{\sigma}_b]_{Shell}} \tag{67}$$

for example if $\lambda = 1$ and $(\bar{\sigma}_b)_P = (\bar{\sigma}_b)_S = (\bar{\sigma}_e)_S = (\bar{\sigma}_e)_P$, then 67 reduces to:

$$(\ell_{cr})_{Shell} \approx 0.76\ (\ell_{cr})_{Plate} \tag{68}$$

This clearly shows that the critical crack length for a spherical shell is less than that of a flat sheet, and as is seen by 67 the ratio depends upon the curvature. This agrees with the statement following equations 39 and 40.

For the special case where $(\bar{\sigma}_b)_P = (\bar{\sigma}_b)_S = (\bar{\sigma}_e)_S = (\bar{\sigma}_e)_P$ we obtain the following expression

$$\left(\frac{\ell_S}{\ell_P}\right)_{cr} = \frac{1}{1 + (0.31 - 0.06\ell n\frac{\lambda}{4})\lambda^2} \tag{69}$$

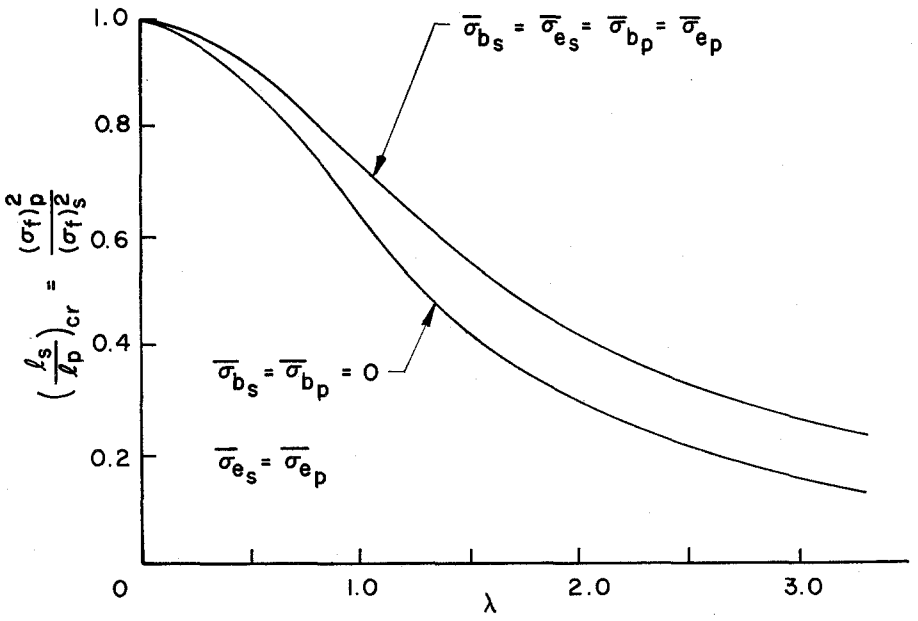

Fig. 4. Square root ratio of critical crack lengths in a spherical cap and a flat plate, for $\nu = 1/3$; $\lambda = \sqrt[4]{12(1-\nu^2)}\ \frac{C}{\sqrt{Rh}}$

This ratio is less than 1 for all $\lambda < 7$. We conjecture that for $\lambda > 7$ the same character will possibly be preserved, but more terms in the basic solution, say up to λ^4, would be required to verify this point. As we have indicated, however, for most practical cases λ is less than 2 hence 69 gives a good approximation. A plot of equation 69 given in fig. 4. This type of behavior was also obtained experimentally, for cracked cylindrical shells, by Sechler and Williams [2].

Returning to equation 66 we note that it can also be written in the form

$$(1 + 0.59\lambda^2)\left(\frac{\bar{\sigma}_e}{\sigma^*_s}\right)^2 - (0.24 + 0.07 \ln\frac{\lambda}{4})\lambda^2 \left(\frac{\bar{\sigma}_e}{\sigma^*_s}\right)\cdot\left(\frac{\bar{\sigma}_b}{\sigma^*_s}\right) + 0.21\,(1 + 0.12\lambda^2)\left(\frac{\bar{\sigma}_b}{\sigma^*_s}\right)^2 = 1 \tag{70}$$

This obviously represents a family of ellipses, which are plotted for different values of the parameter λ, see fig. 5. For λ greater

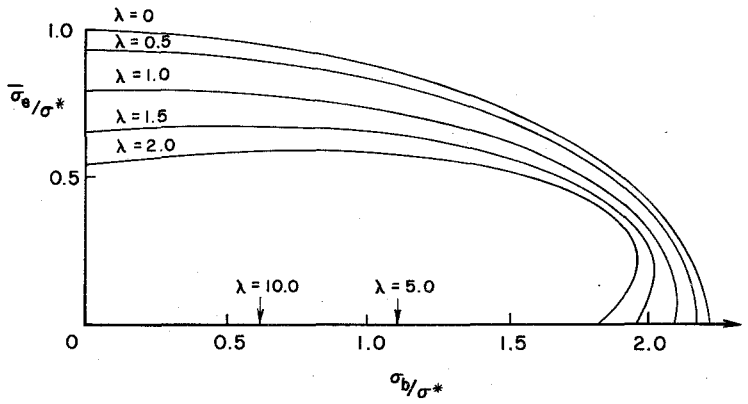

Fig. 5. Extension-bending interaction curve for a spherical cap, for $\nu = 1/3$; $\lambda = \sqrt[4]{12(1-\nu^2)}\,\frac{C}{\sqrt{Rh}}$

than 1.5 we will need higher orders of λ for the determination of the ellipses; therefore for $\lambda = 5$, 10 we show just the intercepts.* It is also clear from fig. 5 that the applied safe load in a cracked spherical shell decreases with a decrease in radius of curvature. For example, if along the crack there is a residual load of equal bending and stretching a flat sheet can carry, before failure occurs, up to a load of $0.88\left(\frac{\bar{\sigma}_e}{\sigma^*}\right)$ while a spherical shell characterized with the parameter $\lambda = 1$ can carry only up to $0.76\left(\frac{\bar{\sigma}_e}{\sigma^*}\right)$, i.e. approximately 14% less load than a flat sheet.

* Curve for $\lambda = 2$ follows the anticipated trend.

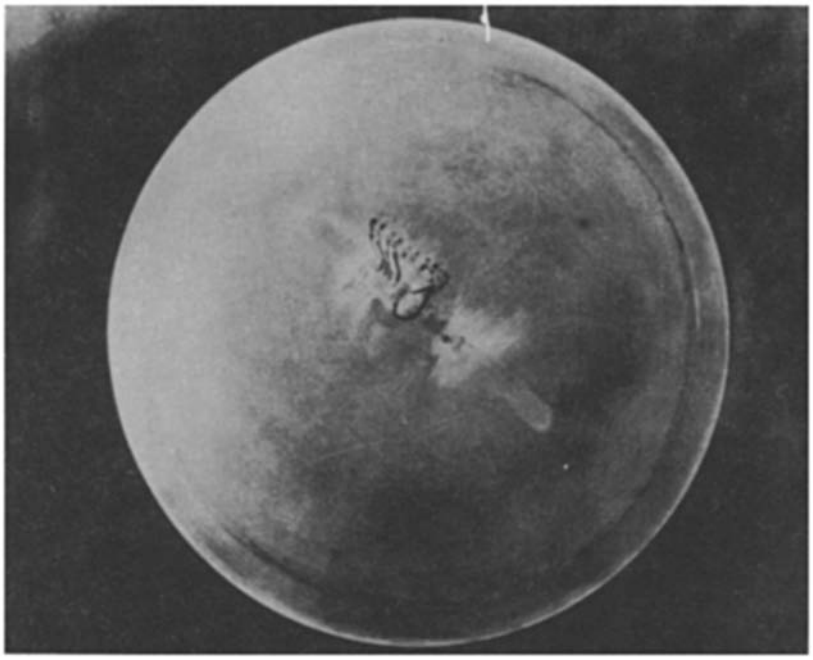

Fig. 6. Spherical cap used for strain measurements.

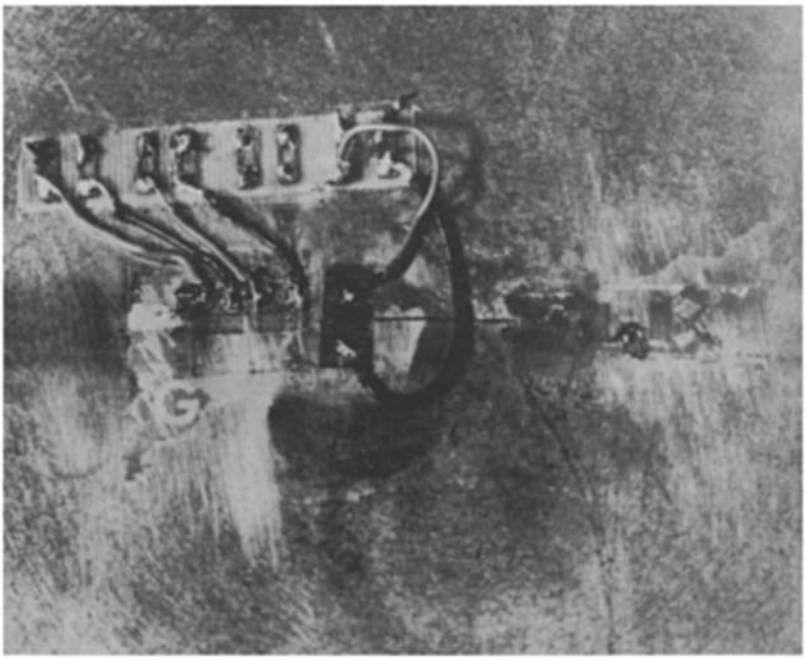

Fig. 7. Close - up of strain gauge locations.

EXPERIMENTAL VERIFICATION

Description of Experiment

To compare theoretical and actual behavior of an initially curved specimen, a preliminary experiment was conducted. We have considered a clamped segment of a shallow spherical shell, containing at the apex a radial cut of length 0.46 in. The shell was subjected to a uniform internal pressure q_o, and the strain ϵ_y at three different positions along the direction of crack propagation was recorded as a function of q_o. The design of the experiment did not permit a determination of critical crack length, furthermore the copper material is too ductile for brittle fracture theory to apply.

Preparations

The shallow shell segment was constructed by the method of "copper electroforming."* Its characteristics were h = 0.009 in., R = 20 in., δ = 0.4 in., $\bar{R}_o$ = 4.25 in., $\nu = \frac{1}{3}$, E = 16 x 10^6 lbs/in^2. A hole of 0.012 in. diameter was drilled at the apex of the shell segment, and a crack was sawed with a jeweler's saw of 0.007 in. thickness. Finally, the ends of the crack were smoothed by the "diamond thread method,"** (diameter of diamond thread less than 0.005 in.). In the process of drilling and of sawing, a wax backing was used in order to avoid damaging of the shell. Next, along the line of crack prolongation, three strain gages were attached on the shell to measure the strains in the Y direction (see figs. 6, 7). The shell was cemented between two circular rings, with $\bar{R}_o$ = 4 in. as the inside radius (see fig. 8). Next the crack was sealed internally with two layers of acetate fibre tape. The first layer was a square of 2 x 2

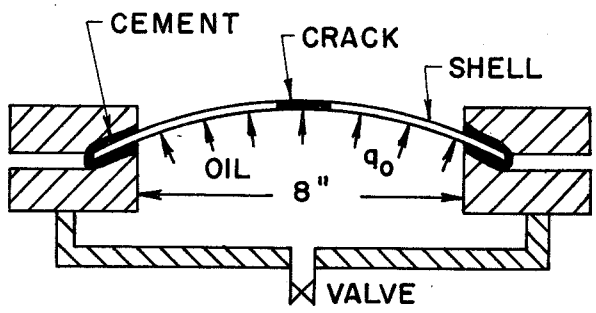

Fig. 8. Schematic of testing apparatus.

inches, and the second layer was a rectangular one of 2 x $\frac{1}{2}$ inches. The following table gives the gage factors and positions of the gages from the crack tip.

Gage no.	G.F.=Gage Factor	X - 1	$\sqrt{\frac{c}{X-1}}$
1	2.10	0.07	1.81
2	2.09	0.29	0.89
3	2.09	0.48	0.69

* See ref. [13].

** A cotton thread impregnated with 6 micron diamond paste.

In fig. 9 we have plotted voltage vs. gage pressure, and because the curves for small pressures were not quite straight lines, a second run was conducted a few hours later. It gave better results (fig. 10). The change between first and second runs is attributed to warming up of the resistance gages in the electronic equipment

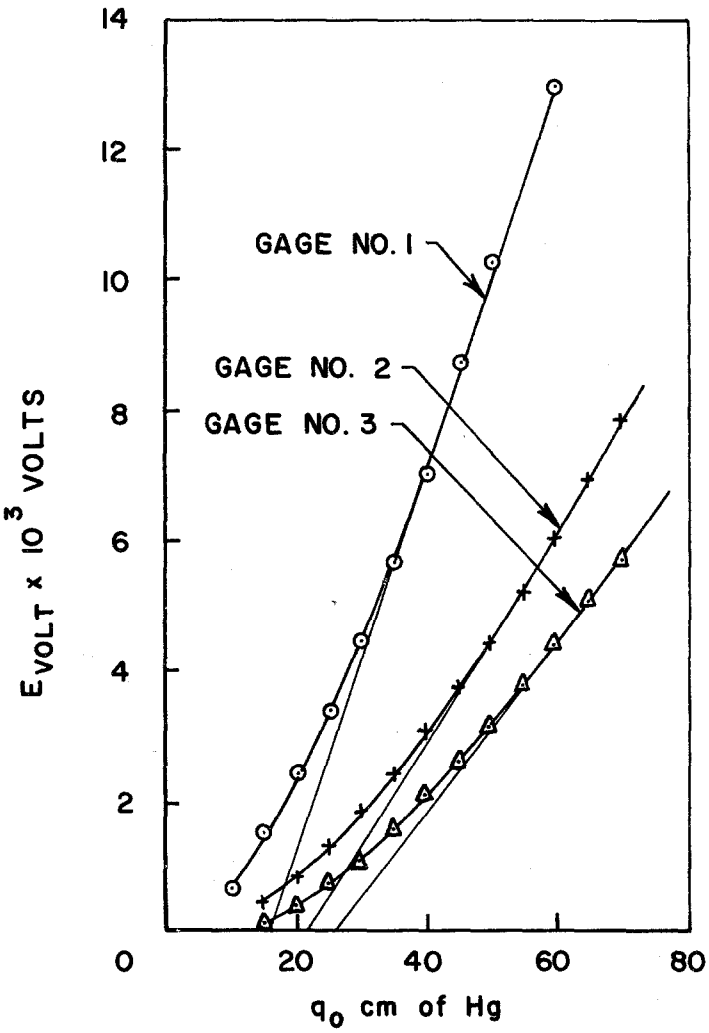

Fig. 9. Test no. 1. Data for a clamped spherical cap containing a crack.

and "setting" of the strain gages. Even for the second run, the curves are slightly curved at the origin. It is possible that the tape carries a small part of the load. In any case, we consider the slope of the curve which is given by

$$C = \text{slope} = \frac{\Delta E_{\text{voltage}}}{\text{A.F.} \times \Delta q_0} \tag{71}$$

where A.F. = amplifier factor = 5. In view of this, we can compute the strains from

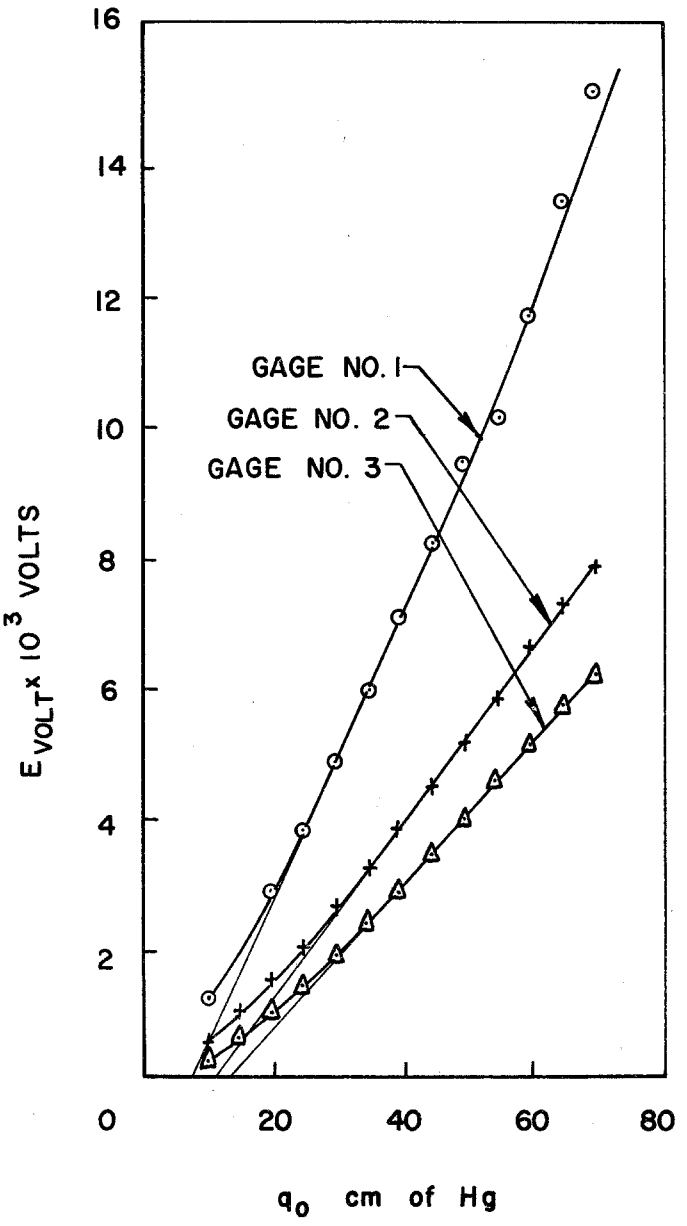

Fig. 10. Test no. 2. Data for a clamped spherical cap containing a crack.

$$\epsilon_{y_{exp}} = \frac{4}{P.S.V.} \frac{Cq_o}{G.F.} \tag{72}$$

Gage No.	Theoretical ε_y	C	Exp. ε_y	C	Exp. ε_y
1	$0.75\times10^{-4}q_o$	3.03×10^{-4}	$0.96\times10^{-4}q_o$	2.42×10^{-4}	$0.77\times10^{-4}q_o$
2	$0.37\times10^{-4}q_o$	1.70×10^{-4}	$0.54\times10^{-4}q_o$	1.37×10^{-4}	$0.44\times10^{-4}q_o$
3	$0.29\times10^{-4}q_o$	1.37×10^{-4}	$0.44\times10^{-4}q_o$	1.15×10^{-4}	$0.36\times10^{-4}q_o$
		first run		second run	

where P.S.V. = Power supply voltage = 6 volts (measured).
The theoretical strains were calculated from equation 43 and the comparison with experimentally determined values follows.

Conclusions

In fig. 11, we compare the theoretical predicted strains with the experimental ones. It is easy to see that close to the crack tip the theoretical results are slightly lower than the experimental ones, e.g. there exists an error of about 3% for the first gage.

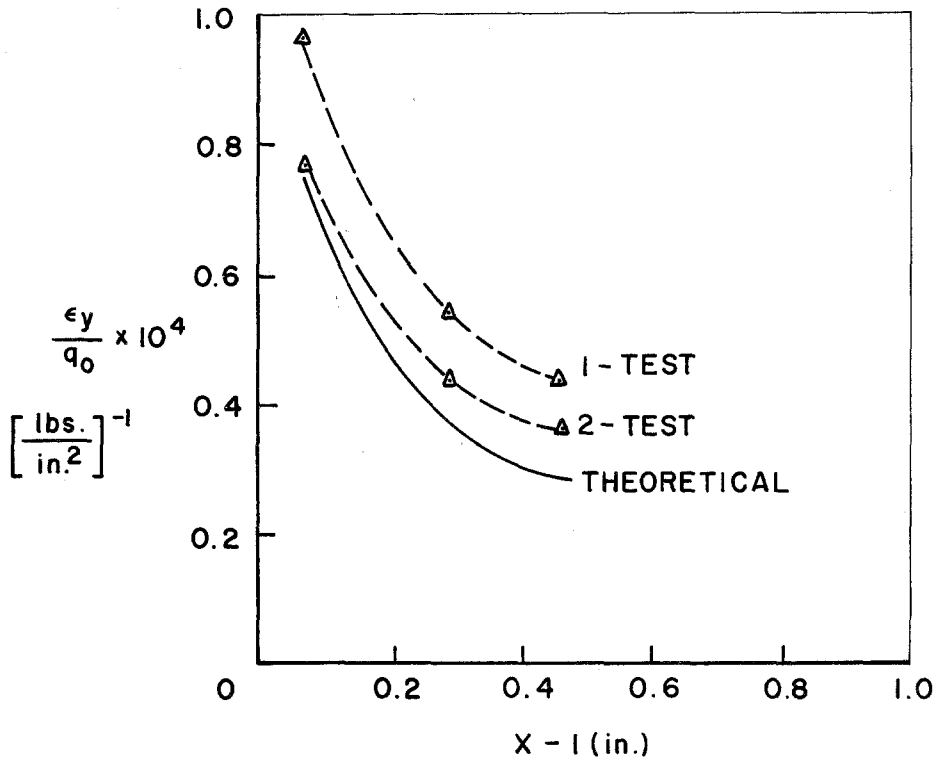

Fig. 11. Comparison of experimental and theoretical strains ahead of the crack.

We recall that in the theoretical formula we neglected terms of $O(\lambda^4)$. This fact could contribute to the difference, as well as the averaging effect of the finite gage thickness. As we move further away from the crack tip the theoretical values become smaller than the experimental ones. This is to be expected, since now ϵ is large and the non-singular terms become significant. Our theoretical results were computed on the basis of only the singular term and furthermore only up to terms of $O(\lambda^2)$.

While it should be pointed out that the bending stresses are practically negligible for this particular test configuration, it was found that on the whole the experimental and theoretical results compare very well.

CONCLUSIONS

The local stresses near the crack point are found to be proportional to $1/\sqrt{\epsilon}$ which is characteristic for crack problems. Furthermore, the angular distribution around the crack tip is exactly the same as that of a flat sheet, and the curvature appears only in the intensity factors and in such a way that for $R \to \infty$ we recover the flat sheet behavior. A typical term is

$$\sigma_{shell} \sim \sigma_{plate} \left\{ 1 + (\text{const} + \text{const}\ \ell n \frac{c}{\sqrt{Rh}}) \frac{c^2}{Rh} + O\left(\frac{1}{R^2}\right) \right\} \tag{73}$$

where the expression in the parentheses is a positive quantity. The general effect of initial curvature, in reference to that of a flat sheet, is to increase the stress in the neighborhood of the crack point. Furthermore, it is of some practical value to be able to correlate flat sheet behavior with that of initially curved specimens. In experimental work on brittle fracture for example, considerable time might be saved since by 73 we would expect to predict the response behavior of curved sheets from flat sheet tests.

The stresses also indicate that there exists an interaction between bending and stretching, i.e. bending loadings will generally produce both bending and stretching stresses, and vice versa.

It is well known that large, thin-walled pressure vessels resemble balloons and like balloons are subject to puncture and explosive loss. For any given material, under a specified stress field due to internal pressure, there will be a crack length in the material which will be self propagating. Crack lengths less than the critical value will cause leakage but not destruction. However, if the critical length is ever reached, either by penetration or by the growth of a small fatigue crack, the explosion and complete loss of the structure occurs. This critical crack length, using Griffith's criterion, was shown to depend upon the stress field, the radius and thickness of the vessel, as well as the material itself (see 64). We were also able to obtain a relation for the ratio critical crack length of a spherical shell over critical crack length of a flat sheet (see eq. 67). In general this ratio is less than unity, which again indicates clearly that a cracked initially curved shell is weaker than a cracked flat sheet subjected to the same loading.

In conclusion it must be emphasized that the classical bending theory has been used in deducing the foregoing results. Hence it is inherent that only the Kirchhoff equivalent shear free condition is satisfied along the crack, and not the vanishing of both individual shearing stresses. While outside the local region the stress distribution should be accurate, one might expect the same type of discrepancy to exist near the crack point as that found by Knowles and Wang [7] in comparing Kirchhoff and Reissner bending results for the flat plate case [8, 9]. In this case the order of the stress singularity remained unchanged but the circumferential distribution around the crack changed so as to be precisely the same as that due to solely extensional loading. Pending further investigation of this effect for initially curved plates, one is tempted to conjecture that the bending amplitude and angular distribution would be the same as that of stretching.

Finally for a clamped spherical shell, the experimental and theoretical strains ϵ_y, at three different locations along the crack prolongation, compare very well.

ACKNOWLEDGMENTS

The author acknowledges several useful discussions of this problem with Professor M. L. Williams and Mr. J. L. Swedlow of the California Institute of Technology. The research reported herein was sponsored in part by the Aerospace Research Laboratories, Office of Aerospace Research of the United States Air Force.

Received June 1964.

REFERENCES

1. Ang, D. D. and Williams, M. L., "Combined Stresses in an Orthotropic Plate Having a Finite Crack," Journal of Applied Mechanics, vol. 28, 1961, pp. 372-378.
2. Sechler, E. E. and Williams, M. L., "The Critical Crack Length in Pressurized, Monocoque Cylinders," Final Report on Contract NAw-6525, California Institute of Technology, September 1959.
3. Reissner, E., "On Some Problems in Shell Theory," Structural Mechanics, Proceedings of the First Symposium on Naval Structural Mechanics, Pergamon Press, 1960, pp. 74-113.
4. Reissner, E., "A Note on Membrane and Bending Stresses in Spherical Shells," J. Soc. Industr. Appl. Math., vol. 4, 1956, pp. 230-240.
5. Folias, Efthymios S., "The Stresses in a Cracked Spherical Shell," (Submitted to the Journal of Mathematics and Physics, 1964).
6. Folias, Efthymios S., "The Stresses in a Spherical Shell Containing a Crack," ARL 64-23, Aerospace Research Laboratories, Office of Aerospace Research, U. S. Air Force, January 1964.
7. Knowles, J. K. and Wang, N. M., "On the Bending of an Elastic Plate Containing a Crack," Journal of Mathematics and Physics, vol. 39, 1960, pp. 223-236.
8. Williams, M.L., "The Bending Stress Distribution at the Base of a Stationary Crack," Journal of Applied Mechanics, vol. 28, Trans. ASME, vol. 83, Series E, 1961, pp. 78-82.
9. Williams, M. L., "On the Stress Distribution at the Base of a Stationary Crack," Journal of Applied Mechanics, vol. 24, March 1957, pp. 109-114.
10. Reissner, E., "Stresses and Small Displacements of Shallow Spherical Shells I, II," Journal of Mathematics and Physics, vol. 25, 1946, pp. 80-85, 279-300.
11. Griffith, A. A., "The Theory of Rupture," Proceedings of the First International Congress of Applied Mechanics, Delft, 1924, pp. 55-63.
12. Swedlow, J. L., "On Griffith's Theory of Fracture," GALCIT SM 63-8, California Institute of Technology, March 1963.
13. Parmerter, R. R., "The Buckling of Clamped Shallow Spherical Shells Under Uniform Pressure," Ph. D. Dissertation, California Institute of Technology, September 1963.
14. Mikhlin, S. G., Integral Equations, English translation by A. H. Armstrong, published by Pergamon Press, 1957.

c	= half crack length
D	$\equiv Eh^3/[12(1-\nu^2)]$ = flexural rigidity
E	= Young's modulus of elasticity
$F(X,Y)$	= stress function
G	= shear modulus
h	= thickness
h^*	= as defined on fig. 3
i	$\equiv \sqrt{-1}$
k	$= \frac{3-\nu}{1+\nu}$
ℓ_s	= 2c = crack length of shell
ℓ_p	= crack length of plate
$(\ell_{cr})_s$	= critical crack length of shell
$(\ell_{cr})_p$	= critical crack length of plate
m_o	= constant as defined in text
M_x, M_y, M_{xy}	= moment components
n_o	= constant as defined in text
N_x, N_y, N_{xy}	= membrane forces
P	= periphery
$q(X,Y)$	= internal pressure
q_o	= uniform internal pressure
r	$= \sqrt{x^2 + y^2}$
r_o	$\equiv \frac{\bar{R}_o}{c}$
R	= radius of curvature of the shell
$\bar{R}$	$\equiv \sqrt{X^2 + Y^2}$
$\bar{R}_o$	= given $\bar{R}$
S	= surface area of the shell
t_o	= constant as defined in text
U	= energy
v_o	= constant as defined in text
V_y	= equivalent shear
$W(X,Y)$	= displacement function
x, y, z	= dimensionless coordinates with respect to the crack length
X, Y, Z	= rectangular cartesian coordinates
α	$\equiv (i)^{\frac{1}{2}}$
β	$\equiv (-i)^{\frac{1}{2}}$
γ	= 0.5768 = Euler's constant

γ^* = surface energy per unit area

δ = height of the shell

$\varepsilon \equiv \sqrt{(\frac{X-1}{c})^2 + (\frac{Y}{c})^2}$

$\varepsilon_x, \varepsilon_y, \varepsilon_z$ = strain components

$\theta = \tan^{-1} \frac{Y}{X}$

$\lambda^4 \equiv \frac{Ehc^4}{R^2D} \equiv \frac{12(1-\nu^2)c^4}{R^2h^2}$

ν = Poisson's ratio

$\nu_o \equiv 1-\nu$

$\rho \equiv \sqrt{\zeta^2 + y^2} = \sqrt{(x-\xi)^2 + y^2}$

$\sigma_{x_b}, \sigma_{y_b}, \tau_{xy_b}$ = bending stress components

$\sigma_{x_e}, \sigma_{y_e}, \tau_{xy_e}$ = stretching stress components

$\bar{\sigma}_x, \bar{\sigma}_y, \bar{\tau}_{xy}$ = applied stress components at the crack

σ_S^* = critical (fracture) stress for shell

σ_P^* = critical (fracture) stress for plate

$\Phi(x,y), \psi(x,y)$ = harmonic functions

$\chi(x,y)$ = deflection of a plate on an elastic foundation.

APPENDIX

The deflection function W and the stress function F are:

$$W(x,y^{\pm}) = \int_0^{\infty} \left\{ P_1 e^{-\sqrt{s^2-i\lambda^2}|y|} + P_2 e^{-\sqrt{s^2+i\lambda^2}|y|} + P_3 e^{-s|y|} \right\} \cos xs\, ds$$

$$F(x,y^{\pm}) = \frac{i\lambda^2 RD}{c^2} \int_0^{\infty} \left\{ P_1 e^{-\sqrt{s^2-i\lambda^2}|y|} - P_2 e^{-\sqrt{s^2+i\lambda^2}|y|} + P_4 e^{-s|y|} \right\} \cos xs\, ds$$

where

$$P_1(s) = \frac{s}{\sqrt{s^2-i\lambda^2}} \{ A_1 J_1(s) + \frac{\lambda^2 A_2}{3} \frac{J_2(s)}{s} + O(\lambda^4) \}$$

$$P_2(s) = \frac{s}{\sqrt{s^2+i\lambda^2}} \{ B_1 J_1(s) + \frac{\lambda^2 B_2}{3} \frac{J_2(s)}{s} + O(\lambda^4) \}$$

$$P_3(s) = -(A_1+B_1) J_1(s) - \frac{\lambda^2 (A_2+B_2)}{3} \frac{J_2(s)}{s} - \frac{i\lambda^2}{\nu_o s^2} (A_1-B_1) J_1(s) + O(\lambda^4)$$

$$P_4(s) = -(A_1-B_1)\,J_1(s) - \frac{\lambda^2(A_2-B_2)}{3}\,\frac{J_2(s)}{s} + O(\lambda^4)$$

where

$$\frac{\lambda^4 RD}{2\sqrt{2}}\,(A_1 + B_1)$$

$$= \frac{n_o c^2}{\sqrt{2}}\left\{1 + \frac{3\pi}{32}\lambda^2\right\} + \frac{m_o\lambda^2\sqrt{EhD}\,c^2}{\sqrt{2}\,(4-\nu_o)}\left\{\frac{13}{32}+\frac{3\gamma}{8}+\frac{3}{16}\,\ell n\,\frac{\lambda^2}{16}\right\}$$

$$+ O(\lambda^4\,\ell n\lambda)$$

$$\frac{\alpha^2\lambda^2}{2\sqrt{2}}\,(A_1-B_1) = -\frac{n_o\,\lambda^2}{\sqrt{2EhD}\,(4-\nu_o)}\left\{\frac{8-7\nu_o}{32} + \frac{4-3\nu_o}{8}\,\gamma + \frac{4-3\nu_o}{16}\,(1+\ell n\,\frac{\lambda^2}{16})\right\}$$

$$+ \frac{m_o}{\sqrt{2}(4-\nu_o)}\left\{1 + \frac{\pi\lambda^2}{32}\,\frac{4-3\nu_o}{4-\nu_o}\right\} + O(\lambda^4\,\ell n\lambda)$$

$$A_2 + B_2 = -\frac{\alpha^2}{8}\,(A_1-B_1)$$

$$A_2 - B_2 = -\left(\frac{4-3\nu_o}{4-\nu_o}\right)\frac{\alpha^2}{24}\,(A_1 + B_1)$$

RÉSUMÉ - On montre que la déformation d'une feuille mince ayant une courbure sphérique initiale, est associée avec celle d'une plaque mince reposant sur une fondation élastique.

En utilisant une forme intégrale, on résoud les équations couplées de Reissner, pour une coque avec une fracture de longueur 2c, pour le plan interne et les contraintes de flexion de Kirchhoff. D'autre part on trouve que la forme explicite des contraintes près due point de fracture, dépend de l'inverse de la demi puissance de la distance, sans dimension, au point ε. Le caractère du champs de contrainte combinée, flexiontension, prêt de l'extrémité de la fracture, est étudié en détail dans le cas particulier d'une fracture radiale dans une calotte sphérique soumise à une pression interne uniforme q_o et qui est encastrée à la limite $\bar{R} = \bar{R}_o$. En attendant une étude complète de la solution, des résultats approchés pour les contraintes combinées de surface, près de l'extrémité de la fracture normale, et le long de la ligne de prolongation de la fracture, ont donnés respectivement

$$\sigma_y(\varepsilon,0) \approx \sigma_x(\varepsilon,0) \approx 0.45\,\sqrt{1/\varepsilon}\,(q_o R/h)$$

ou $\nu = 1/3$, $c = 0.23$ inch, $\bar{R}_o = 4.25$ inch et $\lambda = 0.98$.

Il est interressant de noter que les contraintes σ_x et σ_y le long de la ligne de prolongation de fracture sont égales pour cette géométrie. En général, elles ont le même signe et ne différent légèrement qu'en module, du fait de la composante de flexion. Finalement les résultats expérimentaux et théoriques pour ε_y le long de la ligne de prolongation de la fracture coïncident bien.

ZUSAMMENFASSUNG - Es wird gezeigt, dass die Verformung einer duennen, anfaenglich sphaerisch gekruemmten Platte mit der Verformung einer anfaenglich ebenen Platte, die elastisch

gebettet ist, verbunden ist. Mit Hilfe einer Integralformulation werden die gekuppelten Reissner-Gleichungen fuer eine Schale, die einen Riss der Laenge 2c enthaelt, fuer die ebenen und die Kirchhoff Biegespannungen geloest. Unter anderem wurde festgestellt, dass die explizite Form der Spannungen in der Naehe des Bruchpunktes umgekehrt proportional der Wurzel des dimensionslosen Abstandes vom Punkte ist. Der Charakter des Dehnungs-Biegespannungsfeldes in der Umgebung der Risspitze wird im Detail untersucht fuer den speziellen Fall eines radialen Risses in einer sphaerischen Kappe unter gleichfoermigen Innendruck q_o, die an ihrer Auflage $\bar{R} = \bar{R}_o$ eingeklemmt ist. Die angenaeherten Ergebnisse - das ausfuehrliche Studium der Loesungen ist noch nicht abgeschlossen - fuer die kombinierten Oberflaechenspannungen nahe der Risspitze senkrecht zum Riss und in Richtung des Risses sind von der Form:

$$\sigma_y(\varepsilon,0) \approx \sigma_x(\varepsilon,0) \approx 0.45\sqrt{1/\varepsilon}\,(q_o R/h)$$

et $\nu = 1/3$, $c = 0.23$ inch, $\bar{R}_o = 4.25$ inch und $\lambda = 0.98$.

Es ist interessant, dass die Spannungen σ_x und σ_y entlang der Linie der Rissfortpflanzung gleich sind fuer diessen Fall. Im allgemeinen werden sie dasselbe Vorzeichen haben und sich nur wenig in der absoluten Groesse unterscheiden infolge der Biegekomponente. Die experimentellen und theoretischen Ergebnisse fuer ε_y entlang der Linie der Rissfortpflanzung stimmen sehr gut ueberein.